WIND TUNNEL TEST OF A TWIN, REAR PROPELLER TRANSPORT AIRCRAFT CONFIGURATION AT LOW SPEEDS

Sven-Olof Ridder
The Aeronautical Research Institute of Sweden
Bromma, Sweden

Abstract

Six-component total forces and moments measurements and a limited flow visualization and flow field survey in the propeller region was carried out in a 2 m x 2 m low speed wind tunnel for a twin, rear propeller transport aircraft configuration. The engine nacelles were mounted at the tips of the horizontal tail with the respective propellers in a tractor position.

The experimental parameters studied were: Angles of attack and yaw, angular settings of wing trailing edge flaps, elevator, ailerons and rudder. Also the effect of propeller thrust coefficient with two or one propeller operating or feathered was investigated. The propellers were driven by compressed air motors and the elevator was actuated by an electric servo with the possibility of automatic trim of the pitching moment at different positions of the moment reference point.

The experimental results seem to indicate that propeller thrust effects during twin or single engine operation contribute to stability and are possible to trim with conventional control surfaces. At angles of attack up to the stalling of the wing the propellers are operating in an air stream with no loss of total head and rather modest angular distortion.

I. Introduction

For multi-engined propeller transport aircraft the arrangement with wing mounted engines and the propellers in a tractor position has become the accepted standard solution. The principal merit of this well established configuration is that the weight of the propulsive system is disposed in such a way that is favourable for a low weight of the airframe and for the center of gravity problem of the aircraft.

The principal disadvantages associated with the conventional layout are the high yawing and rolling moments in the critical engine out condition. Also the reduction in pitch stability due to slipstream effects poses problems. An additional disadvantage is the propeller that is mounted close to the passenger cabin, causing a need for extensive sound proofing for acceptable cabin noise levels.

The conventional transport configuration was evolved during the piston engine era when comparatively high cabin noise and vibration levels had to be accepted. With gas turbines the weight of the propulsive system is reduced considerably and for the next generation of passenger carrying aircraft a low cabin noise level will be a prime objective. For these reasons and others it might be argued that a rear engine and a propeller position would be feasable from a technical point of view and have more passenger appeal for future propeller aircraft.

Most rear propeller aircraft are designed as pushers. This propeller position has its inherent problems with the propeller blades crossing the wakes from the tailplane and/or the wing, an interference that usually is associated with elevated propeller noise levels. Another typical disadvantage of the pusher is the ground clearance problems. The pusher propeller also to some extent cancels the control surface effectiveness of the tail.

Most of the above problems could be avoided if the propellers are mounted in a tractor position on the tailplane. For a twin-engined configuration the natural choice would be to mount the engines on the horizontal tail. The engine position for the configuration of the present study is at the tips of the horizontal tail. In this position the "wetted" surface immersed in the propeller slipstream is minimized. With the wing in a low position on the fuselage the horizontal tail is mounted high on the rear fuselage with 10^{o} of dihedral in order to get the propeller disc plane above the wing wake.

The reason for initiating the present wind tunnel study was to get basic information on the particular aerodynamic characteristics of this type of aircraft configuration. The geometry of the wind tunnel model is shown in the three view drawing of Fig.1 and the photograph in Fig.2. The proportions of the model should be representative of a transport aircraft for about 100 passengers.

2. Model and Test Equipment

Wing Section

The wind tunnel testing was carried out in the low speed wind tunnel L2 at KTH in Stockholm. The size of the test section is 2 m × 2 m. The wing of the model has a high aspect ratio, and with a span of 1.5 m the wing tip chord was about 0.06 m. Assuming a test section wind speed of 40 m/s the tip section Reynolds number will be about $0.16 \cdot 10^6$.

The object of the experimental study was to establish the effects of propulsion on the aerodynamic characteristics, e.g. on stability and trim. In order to clearly sort out these effects it was desirable that the basic aerodynamics of the model in the wind tunnel would reasonably well correlate with a hypothetical full scale aircraft. The wind tunnel model was not a scale model of a new project and hence true geometrical reproduction was not important.

The wing section chosen for the model is shown in Fig.3. The intention was that this section should give the wing a fairly long, straight part of the lift and pitching moment curve, as well as a reasonably high stalling angle and maximum lift at even very low Reynolds numbers. The wing was mounted on the fuselage with the same zero lift direction as the hypothetical full scale wing. Also the vertical position of the wing trailing edge was retained in order to reproduce the position of the wing wake. The wing was fitted with a single slotted trailing edge flap set at 10° and 30° to represent take-off and landing configurations respectively.

Engine and Propellers

The engines were obtained from a manufacturer of compressed air tools. During the wind tunnel tests the engines were fed with compressed air of several times the normal operating pressure. In this way it was possible to extract about 5 horsepower from each engine without seriously reducing their useful service life.

The rotational speed of each engine was governed by a remotely actuated throttle valve installed in the model. This system gave individual control of the speed including the shut down of the two engines.

The propellers used were six-bladed model aircraft propellers with a hub that permitted setting of the desired blade angle. The basic propellers had a diameter of 0.25 m that was cut down to 0.20 m for the wind tunnel tests. The blade angle setting used was 38° at the 75% radius blade station.

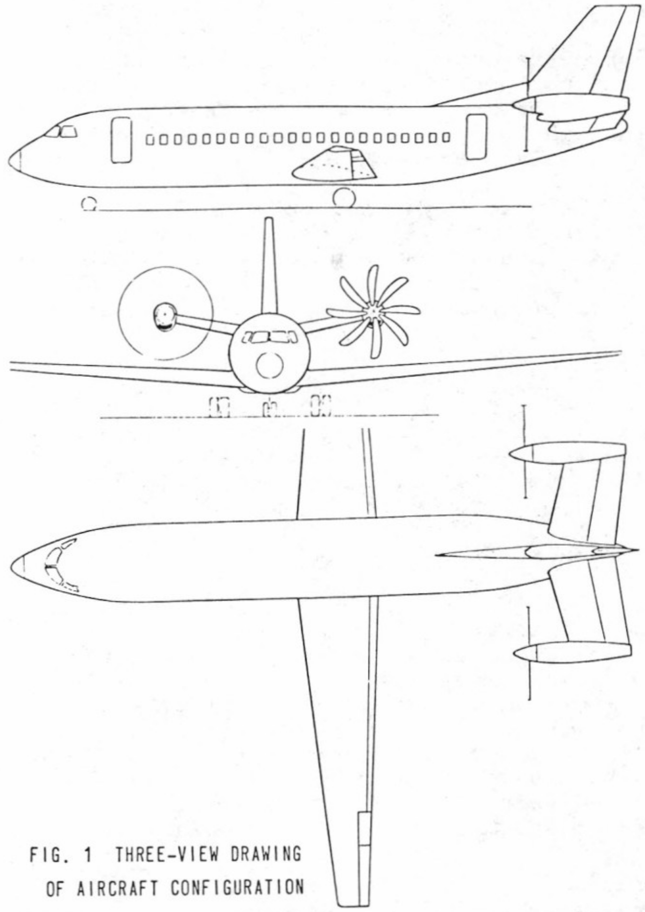

FIG. 1 THREE-VIEW DRAWING OF AIRCRAFT CONFIGURATION

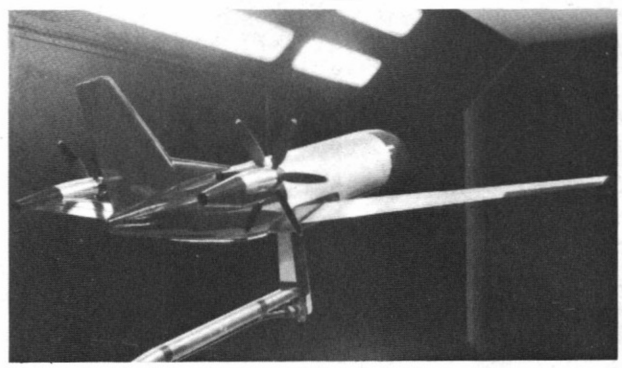

FIG. 2 PHOTOGRAPH OF WIND TUNNEL MODEL

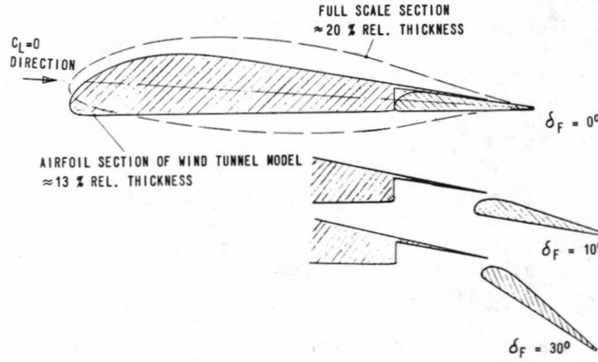

FIG. 3 WING AIRFOIL SECTION OF WIND TUNNEL MODEL

Balance and Autotrim System

The balance used was of the internal six-component strain gauge type with provisions for the feeding of compressed air through integral drillings in the center of the balance frame.

The elevator angle could be remotely controlled by an electric servo system with indication of the angular position. The system could either be used to set the desired elevator angle for a new test run or be used as an automatic trimming device to keep the pitching moment zero during the test run.

The other control surfaces and wing flaps had conventional brackets for manual changes of settings. The model was built in a suitable mixture of metal and composites by members of the laboratory staff.

Special Flow Field Survey Probes

The wing wake was measured by means of a simple total head probe and a vertical traversing mechanism that could be mounted at various spanwise stations. The propeller slipstream was traversed radially with a total head and static pressure probe that alignes automatically with the local flow direction. This device reads the swirl angle directly and also gives reliable pressure data at large angular flow deviations.

Data Acquisition System

The balance and probe recordings were processed by a SEL 32 digital computer that also monitored the various subsystems in the test setup. The angle of attack was corrected for upwash due to test section wall interference and for balance and support deflections.

3. Conduction of Tests

The balance readings were generally recorded during continuous change of angle of attack or angle of yaw. The other test parameters, e.g. dynamic pressure, propeller rotational speed, flap setting being constant. One exception from this routine was when the autotrim device was activated to continuously trim out the pitching moment.

In the preliminary test both increasing and decreasing angle of attack runs were made to check effects of aerodynamic lag as well as possible lag in the recording system.

4. Test Program

In the first part of the experimental program, as put forward in the present context, the emphasis was on the acquisition of longitudinal aerodynamic data. Only a few lateral test series were run.

The effects of propulsion were investigated for four different conditions: 1) Propeller off, 2) Propeller feathered, 3) n = 10600 rpm corresponding to a thrust coefficient of $C_F \approx 0.25$ or a second segment climb angle of about 6^o with both engines operating, and 4) n = 13000 rpm corresponding to $C_F \approx 0.50$ or a climb angle of about 16^o, both engines operating.

The forces and moments measurements were supplemented by various flow field surveys using pressure probes and flow direction indicators. The normal tests section dynamic pressure was 100 mm H_2O corresponding to approximately 40 m/s.

5. Test Results

Reynolds Number Effects (Figs 4 a-c)

The lift curves at different values of test section dynamic pressure clearly shows that there is a critical value between 40 and 50 mm H_2O corresponding to a tip section Reynolds number of about $0.12 \cdot 10^6$. The lift curves are fairly linear indicating no significant progressive trailing edge separation prior to the stalling of the wing. The kink in the lift curves for zero flap deflection could be removed by the addition of a small vortex generator at the wing root fillet.

The main effect of an increase in Reynolds number above the critical value is to improve the lift in the post stall regime. The conclusion should be that increased Reynolds number in the first place stabilizes the flow in the forward part of the wing section probably by influencing the length of the laminar separation bubble.

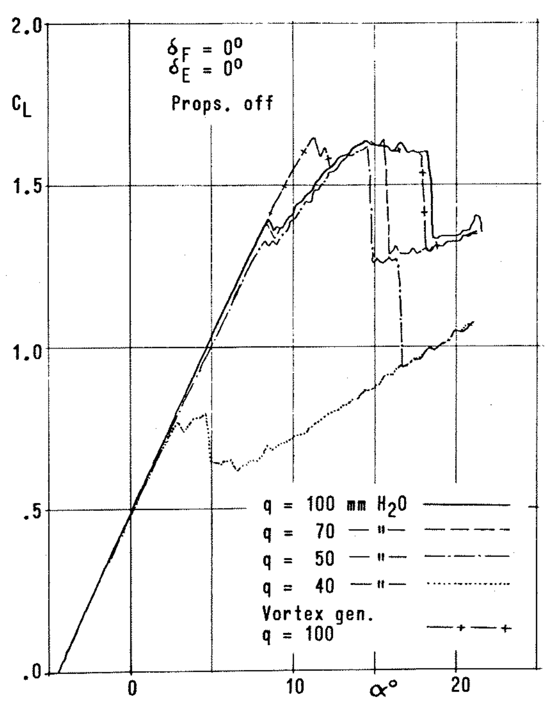

FIG. 4,a EFFECTS OF REYNOLDS NUMBER ON LIFT CURVE, $\delta_F=0^o$

The effects of Reynolds number are similar for the different flap settings. The C_{Lmax} values and stalling angles of the wind tunnel model are reasonably close to the full scale values to be expected from an aircraft of this general type. Thus it should be justified to assume that the rather low Reynolds number wind tunnel tests should form a representative basis for the ensuing study of propulsion effects.

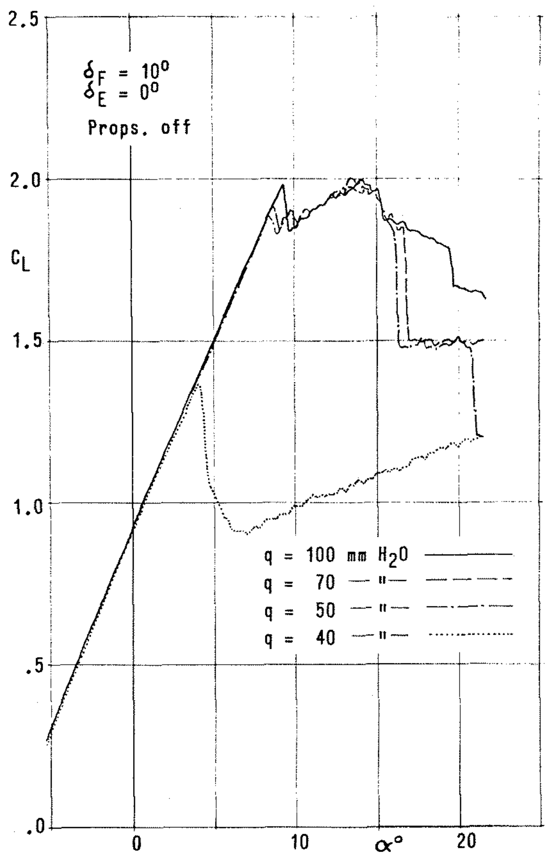

FIG. 4,b EFFECTS OF REYNOLDS NUMBER ON LIFT CURVE, δ_F=10°

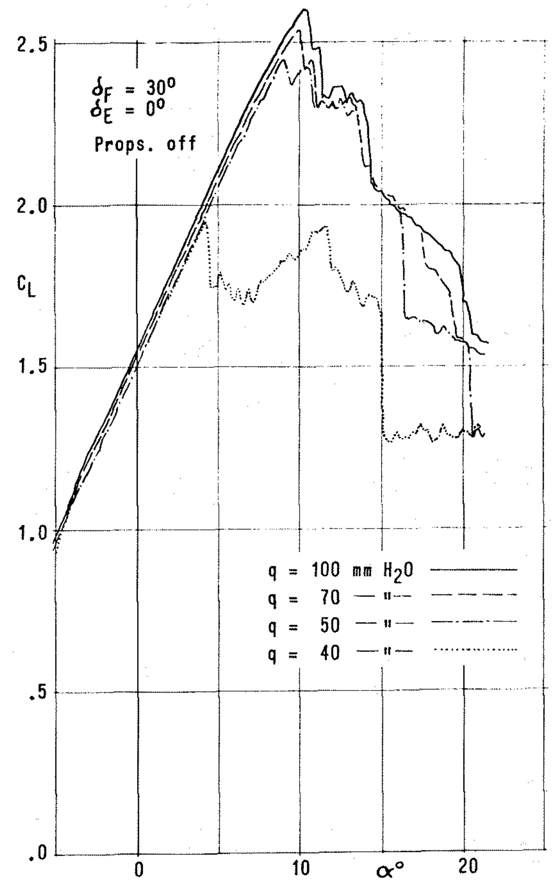

FIG. 4,c EFFECTS OF REYNOLDS NUMBER ON LIFT CURVE, δ_F=30°

Effects of Symmetric Propulsion (Figs 5 a-d)

The obvious effects of increasing propeller thrust is an increase in lift curve slope and pitch stability. The latter effect is more pronounced which means that positive propulsion moves the neutral point of the configuration rearwards. At the maximum value of thrust coefficient ($C_F \approx 0.5$) the displacement of NP is about 5% MAC.

The magnitude of the lift increase is roughly of the order of twice the direct lifting component of the axial propeller thrust. This indicates that some jet blowing slipstream effect is present.

The effect of propulsion on the pitching moment is in a nose down direction as could be expected from the comparatively high position of the thrust line. This effect is slightly lower than could be calculated from the direct axial propeller thrust line force.

As a consequence of these two effects on lift and pitching moment the effect of propulsion for trimmed conditions will be partly cancelled as is shown in the diagram of Fig.5 d.

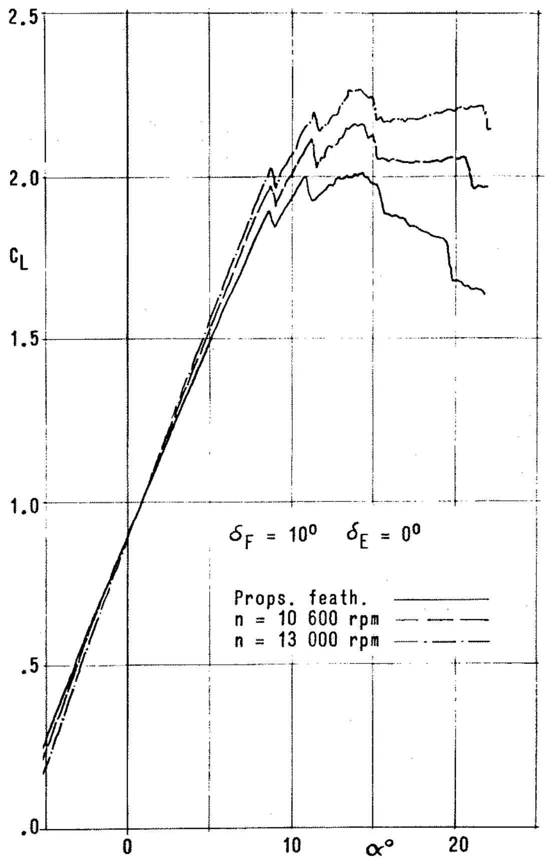

FIG. 5,a EFFECTS OF SYMMETRIC PROPELLER THRUST, $C_L(\alpha)$

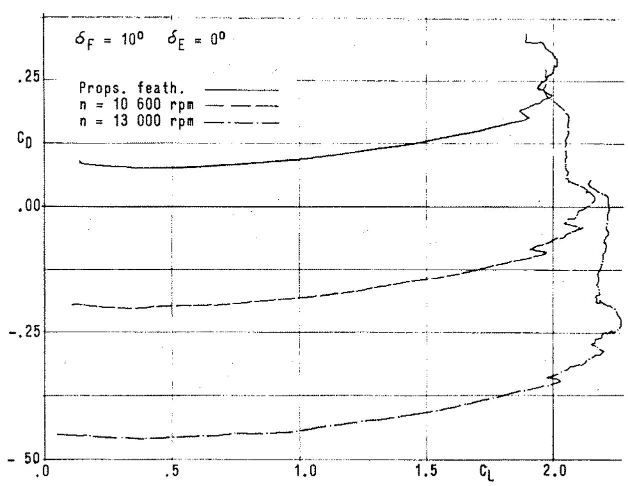

FIG. 5,b EFFECTS OF SYMMETRIC PROPELLER THRUST, $C_D(C_L)$

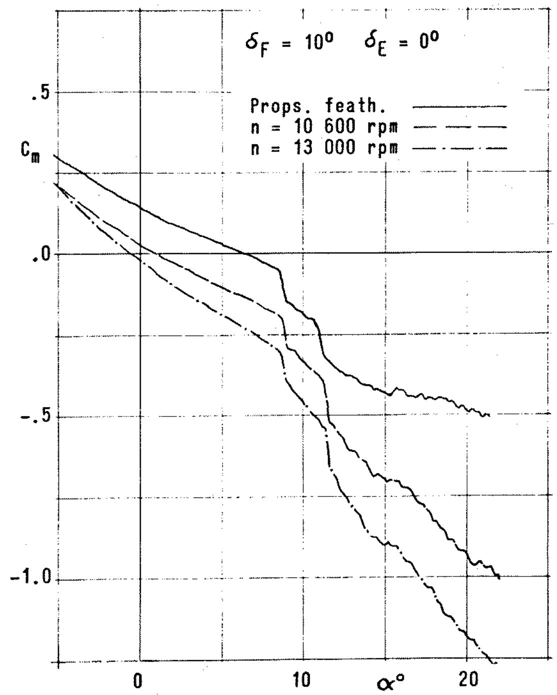

FIG. 5,c EFFECTS OF SYMMETRIC PROPELLER THRUST, $C_m(\alpha)$

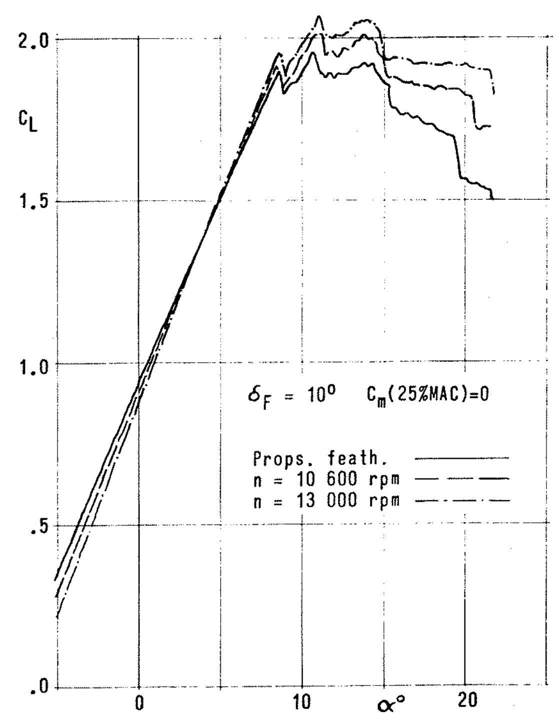

FIG. 5,d EFFECTS OF SYMM. PROPELLER THRUST, $C_L(C_m=0)$

Analysis of Slipstream Induced Increase in Pitch Stability (Fig.6)

The nature of the slipstream induced increase in pitch stability is analysed in the following way. Three different wing off configurations were tested, one with tail off (fuselage only), a second with tail and nacelles on but with propellers off and a third configuration with both propellers operating at 13000 rpm. The lift and moment data for the three different model configurations are presented in Fig.6. For clarity all curves are displaced vertically to intersect at zero angle of attack.

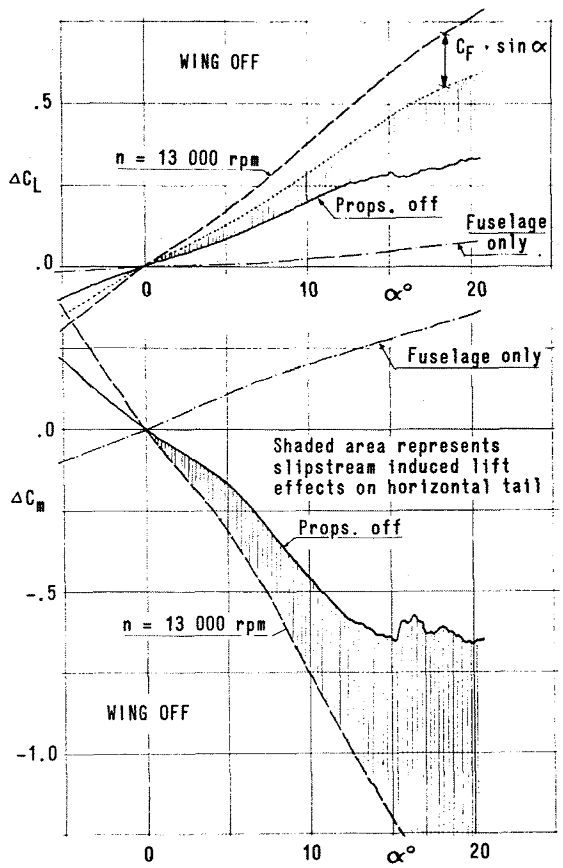

FIG. 6 ANALYSIS OF SLIPSTREAM INDUCED INCREASE IN PITCH STABILITY.

The direct lift component $C_F \cdot \sin\alpha$ of the propeller thrust is subtracted from the lift of the powered configuration. The shaded area then represents the slipstream induced lift on the horizontal tail (and the lifting component on the propellers). The effect of the slipstream is an increase in both the lift and pitching moment from the horizontal tail of about 50% at angles of attack up to 10°. At higher AOA the amplifying effect of the slipstream is still more pronounced, probably because of the suppression of flow separations on the horizontal tail.

The stabilizing effect of the slipstream can be adequately explaind by its jet blowing effect on the horizontal tail which increases the lift curve slope of the immersed aerodynamic surface.

Effects of Symmetric Propeller Thrust on Elevator Effectiveness and Trim Changes (Figs 7 a-b)

In Fig.7a is presented the increase in elevator effectiveness due to slipstream. This increase is about 27% at the higher value of thrust coefficient for moderate (-10°) of elevator deflection. At -20° of elevator deflection the capability to trim does not increase linearly with the angle of the control surface which indicates the presence of flow separations.

The effect of slipstream could perhaps be expected to clear up the flow separations and improve the linearity of the control surface. According to test results, however, the opposite effect seems to occur. The increase in elevator effectiveness due to slipstream is only about 11% for the larger elevator deflection.

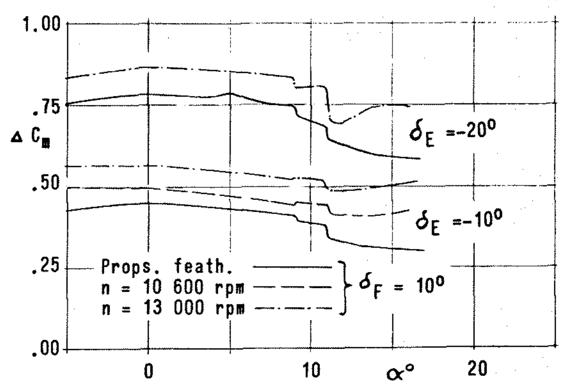

FIG. 7,a EFFECTS OF SYMMETRIC PROPELLER THRUST ON ELEVATOR EFFECTIVENESS.

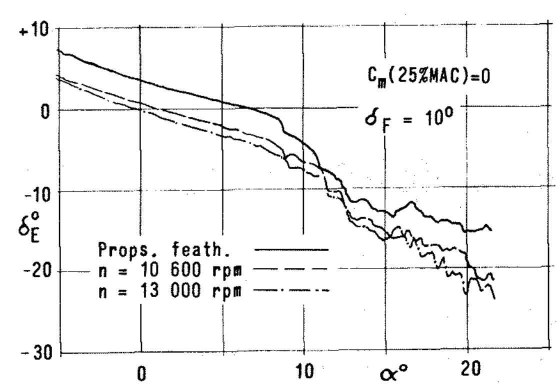

FIG. 7,b EFFECTS OF SYMMETRIC PROPELLER THRUST ON TRIM CHANGE.

The combined effects of the slipstream on both pitch stability and elevator effectiveness is best demonstrated by the trim curves in Fig.7b. In this diagram are shown the elevator angles required for trimming the pitching moment versus AOA for different values of propeller thrust coefficient.

It is evident that the trim changes are comparatively mild with regards to the high propeller thrust line, especially in the range of C_F from 0.25 to 0.50.

Effects of Asymmetric Propeller Thrust Figs 8 a-c)

The effect of asymmetric propeller thrust on longitudinal aerodynamics is presented for three different propulsive cases. The first reference case is with n = 10 600 rpm for both propellers, the second is with the starboard propeller feathered and the port propeller running at 13 000 rpm, and the third case vice versa.

From Fig.8b it is evident that for the three cases the total propeller thrust is roughly the same. The effect of starboard or port engine running is quite evident on lift, but is very pronounced on the pitching moment, Fig.8c.

This effect must be attributed to the influence of slipstream rotation. Both propellers are right hand propellers. The horizontal tail will only reduce the slipstream rotation in a limited sector as it only passes through half the slipstream.

The effect of this partially inhibited slipstream rotation can be interpreted as a change in the resultant thrust vector direction by the interaction from the horizontal tail. From both the effects on lift and pitching moment is evident that this change of resultant thrust vector is of the order of $\pm10^{o}$ in a vertical plane

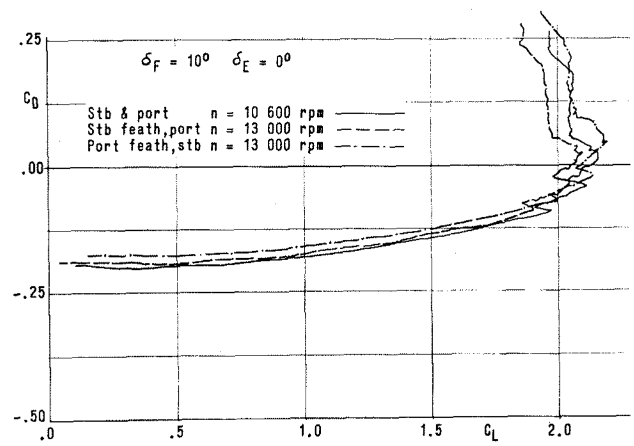

FIG. 8,b EFFECTS OF ASYMMETRIC PROPELLER THRUST, $C_D(C_L)$

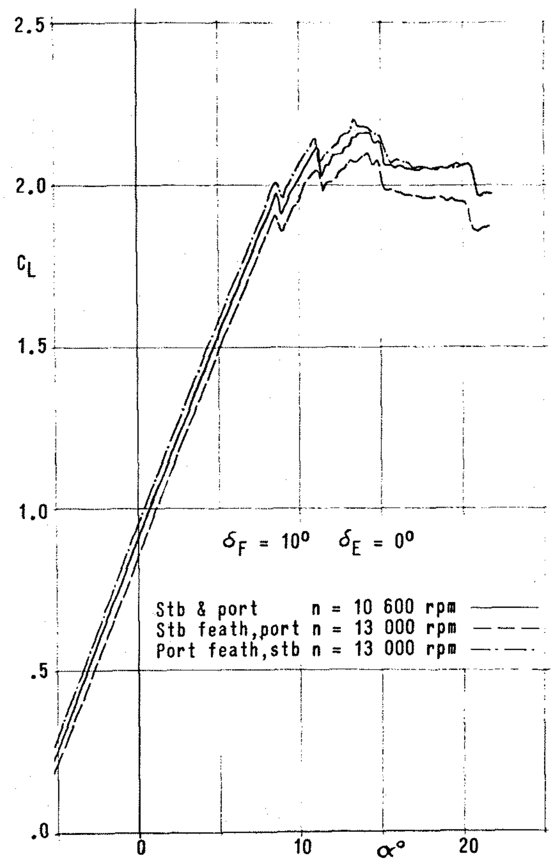

Fig. 8,a EFFECTS OF ASYMMETRIC PROPELLER THRUST, $C_L(\alpha)$

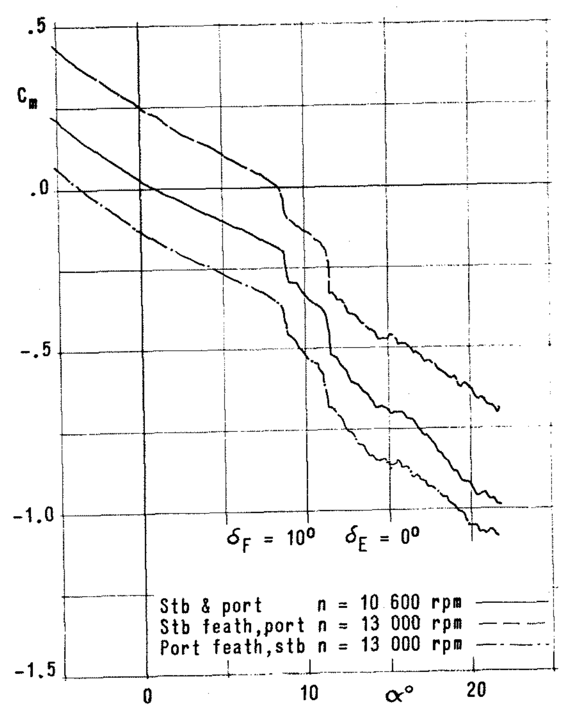

FIG. 8,c EFFECTS OF ASYMMETRIC PROPELLER THRUST, $C_m(\alpha)$

Effects of Symmetric Propeller Thrust on Lateral Characteristics (Figs 9 a-b)

The effect of propeller thrust on the rolling moment is presented in Fig.9a. The rolling moment is of opposite sign of the propeller shaft torque as could be expected, but about 2 to 3 times higher than the estimated shaft torque value.

The corresponding "vectoring" of the resultant propeller thrust, if assumed to pass through the center of the disc, is of the order of ±15°. This value is 50% higher than the corresponding value derived from the pitching moment data of Fig.8c. The difference could be explained by the fact that the part of the slipstream that is not influenced by the straightening effect of the horizontal tail has more leverage than the distance from propeller center to fuselage center line.

In the diagram of Fig.9a is also shown the rolling moment obtained by an aileron deflection of ±10°. From this measure of aileron efficiency it can be concluded that the rolling moment from the propeller thrust requires about ±7° of aileron deflection for compensation. This aileron loading with both engines running is probably unacceptably high.

The effect of propeller thrust on the yawing moment is shown in Fig.9b. The influence is less pronounced than that on the rolling moment. This value of yawing moment corresponds to a lateral displacement of the axial propeller thrust by 20% of the propeller blade radius.

The effect on the yawing moment can to some extent be explained by the dihedral angle (10°) of the horizontal tail. The yawing moment requires a rudder deflection of slightly less than 4° for compensation at $\beta = 0°$. The effect of slipstream is also to increase the yaw stability about 30%.

Schematic Presentation of Propeller Thrust Effects (Fig.10)

The propeller thrust effects presented as a displacement and a turning of the nominal axial thrust vector is shown in Fig.10. These effects should mainly be attributed to the interference of the horizontal tail with part of the rotating slipstream.

For clarity also the required control surface deflections are indicated. With respect to maximum engine out yawing moment the starboard engine should be critical with right hand rotating propellers.

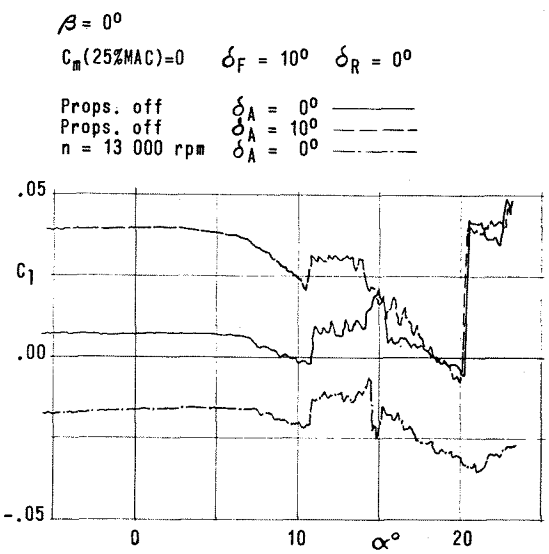

FIG. 9,a EFFECTS OF SYMMETRIC PROPELLER THRUST ON LATERAL CHARACTERISTICS, $C_l(\alpha)$

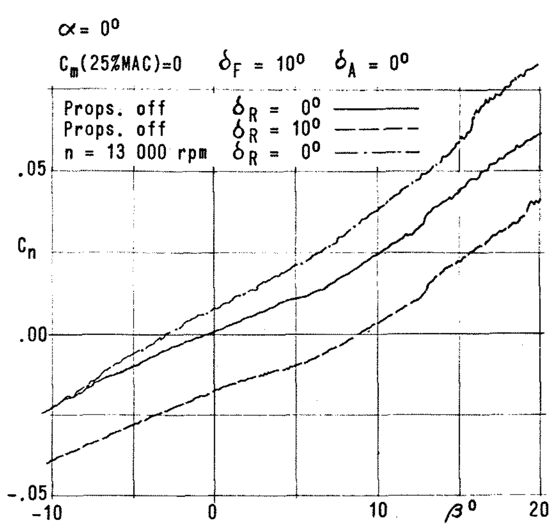

FIG. 9,b EFFECTS OF SYMMETRIC PROPELLER THRUST ON LATERAL CHARACTERISTICS, $C_n(\beta)$

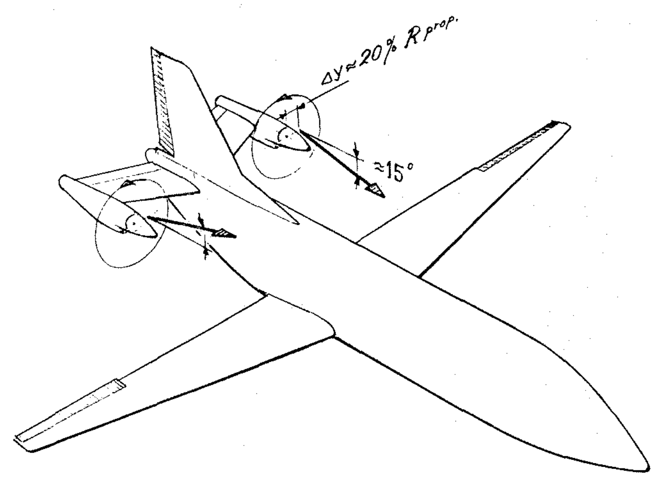

Right hand prop.rot. — Stb-engine critical

FIG. 10 SCHEMATIC PRESENTATION OF PROPELLER THRUST EFFECTS.

Propeller Slipstream Flow Field Surveys (Figs 11 a-b)

The increase in stagnation pressure behind the propeller is shown in Fig.11a, at three different stations in the slipstream and for three different propeller operating conditions. It is evident that the inner part of the propeller blade is not working to satisfaction, probably due to both unsuitable blade twist and poor airfoil section in this area.

The negative pressures measured in the tip region are presumably caused by disturbances from the low static pressure in the cores of the tip vortices.

In Fig.11b the propeller slipstream swirl angle is presented. During these measurements the engine nacelle was mounted on an extension to move the propeller a considerable distance upstream the horizontal tail. The measurement should be representative of a free propeller.

There is a correspondence between low increase in stagnation pressure and low swirl angle as is to be expected. The mean value of the swirl angle on the active part of the slipstream is of the order of

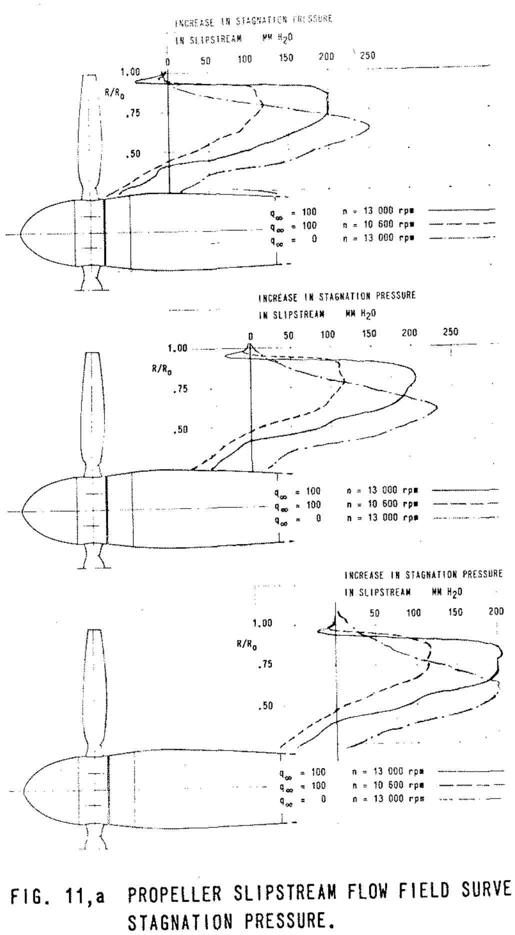

FIG. 11,a PROPELLER SLIPSTREAM FLOW FIELD SURVEYS, STAGNATION PRESSURE.

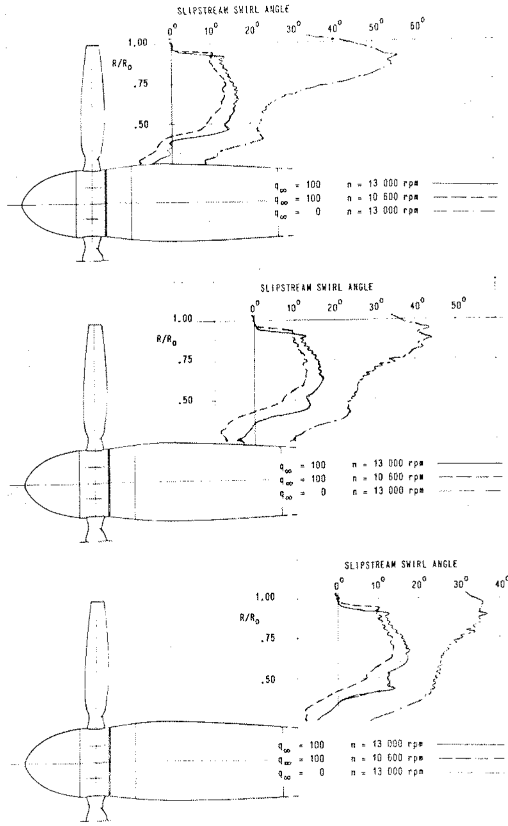

FIG. 11,b PROPELLER SLIPSTREAM FLOW FIELD SURVEYS, SWIRL ANGLE.

15^o. This angle is somewhat smaller than what could have been anticipated from the comparatively high calculated values of the turning angle of the effective propeller thrust vector.

As a matter of curiosity the very high swirl angles for the static condition can be noted. It should be pointed out, however, that the highest values are measured in the induced viscous flow in the mixing region outside the slipstream proper.

Wing Wake Vertical Position in the Propeller Disc Plane (Figs 12 a-b)

The wing wake, if interfering with the propeller, might cause problems such as increased propeller noise, reduced fatigue life, etc. The present configuration was laid out in such a way as to hopefully avoid such an interference.

In Fig.12a are presented the results of wing wake surveys in the propeller disc plane with retracted flaps. The measurements were carried out with propellers off, and indicate an ample clearance between wing wake and propeller for pre-stall angles of attack. At the stalling of the wing the propeller will be partly immersed in the separated wake flow.

With flaps extended 30°, as shown in Fig.12b, the wake is substantially lower, but flows also in this case into the propeller disc when the wing stalls.

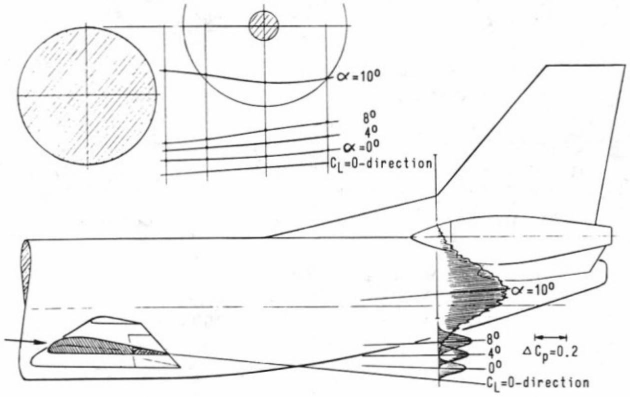

FIG. 12,a WING WAKE VERTICAL POSITION IN THE PROPELLER DISC PLANE, $\delta_F=0^\circ$

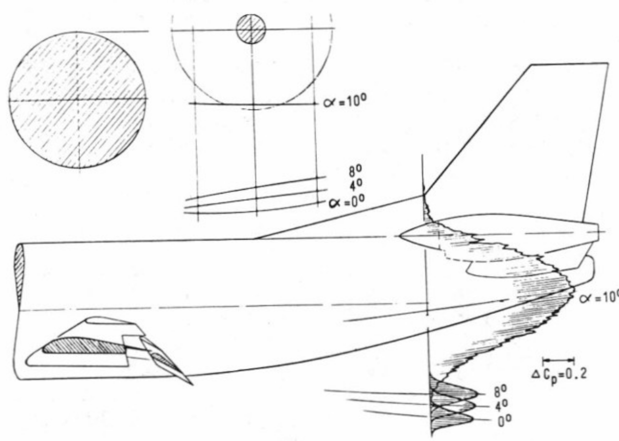

FIG. 12,b WING WAKE VERTICAL POSITION IN THE PROPELLER DISC PLANE, $\delta_F=30^\circ$

Photographs of Flow Angle Visualization in the Propeller Disc Plane (Figs 13,14

The local flow angle at the propeller was visualized using an arrangement with small pieces of balsa wood suspended on thin wires. The rim of the propeller disc was also indicated by a circular wire.

In Fig.13a, with retracted flaps and $\alpha = 0^\circ$ (cruising condition), it can be seen that there is a slight downwash (of the order of 2-4 degrees). In Fig.13b, with $\alpha = 10^\circ$, the effect of wing stalling can be seen in the lower part of the propeller disc where the balsa rods oscillate.

In Fig.14a, with $\delta_F=10^\circ$ and $\alpha = 4^\circ$ (second segment climb condition), the flow directions in relation to the propeller shaft seems so be about the same as in Fig.13a (cruise condition). In Fig.14b, with $\delta_F=30^\circ$ and $\alpha = 0^\circ$ (approach condition), the relative downwash is more pronounced (of the order of 6-8 degrees).

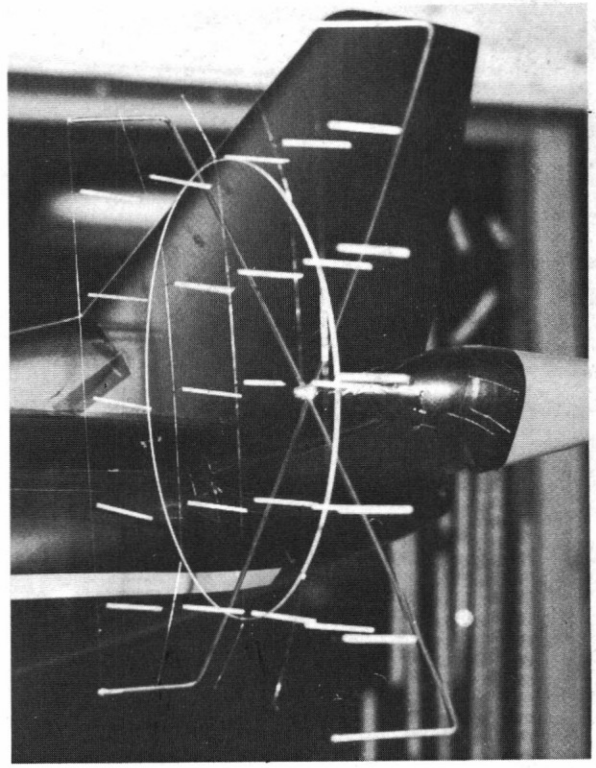

FIG. 13,a FLOW ANGLE VISUALIZATION IN THE PROPELLER DISC PLANE, $\alpha=0^\circ$ $\delta_F=0^\circ$

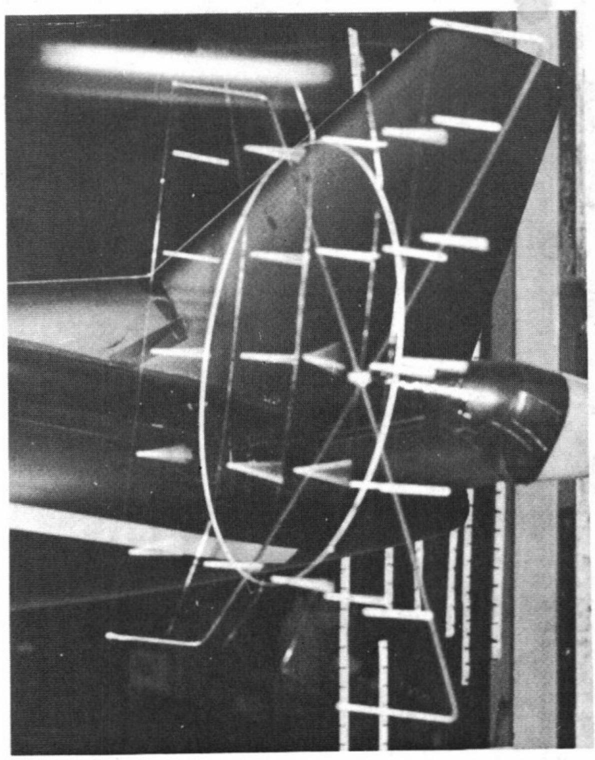

FIG. 13,b FLOW ANGLE VISUALIZATION IN THE PROPELLER DISC PLANE, $\alpha=10^\circ$ $\delta_F=0^\circ$

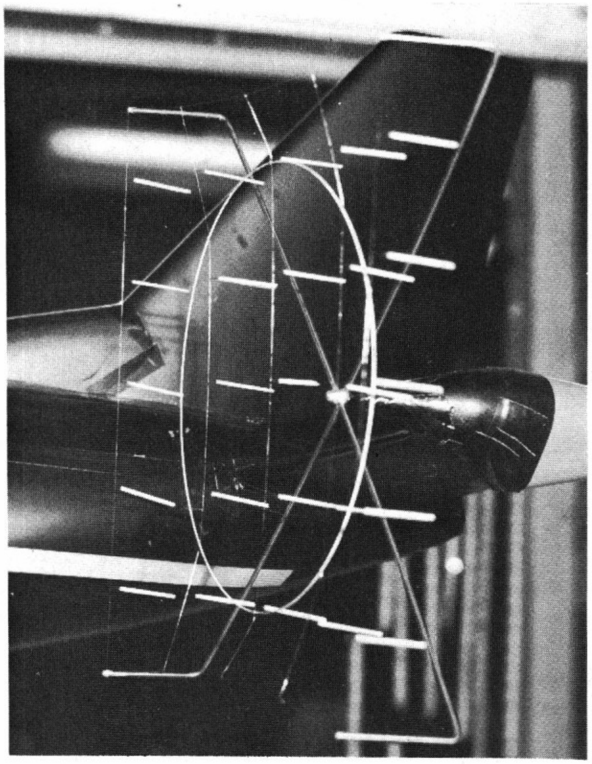

FIG. 14,a FLOW ANGLE VISUALIZATION IN THE PROPELLER DISC PLANE, $\alpha = 4^0$ $\delta_F = 10^0$

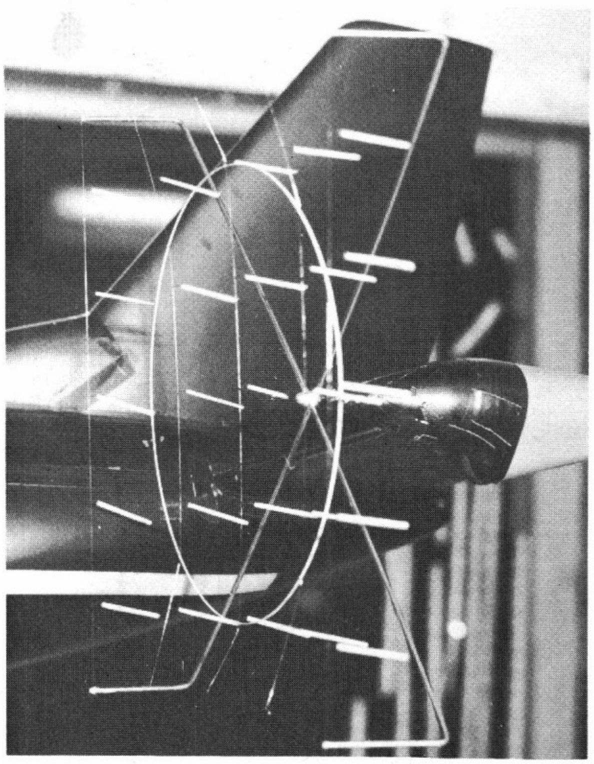

FIG. 14,b FLOW ANGLE VISUALIZATION IN THE PROPELLER DISC PLANE, $\alpha = 0^0$ $\delta_F = 30^0$

6. Conclusions

From a wind tunnel study of the basic aerodynamic problems of a rear propeller, twin engine transport aircraft configuration the following conclusions are made.

- The propulsive propeller slipstream increases the static stability in pitch and yaw as well as the elevator effectiveness appreciably and the lift curve slope and maximum lift slightly.
- The comparatively high propeller thrust line creates a nose down pitching moment, but trim change effects due to change of power setting seem to be moderate.
- With both engines running there is a pronounced rolling moment and an appreciable yawing moment that mainly is caused by the interference of the slipstream from the co-rotating propellers with the horizontal tail (effects of slipstream rotation).
- The same phenomenon creates a marked change in pitching moment from the stopping of either engine (nose up or nose down).
- In the normal (pre-stall) angle of attack range the propellers are working with adequate margin to the wing wake, and the angular flow distortions at the propeller disc due to wing downwash and angle of attack seem to partly cancel at normal operating conditions.
- With a suitable wing section for the wind tunnel model, exploratory tests can be carried out at low Reynolds numbers.
- Reasonably correct representation of the structure of the propeller slipstream is essential during testing, especially slipstream swirl angles.

Symbols and Definitions

A	Wing aspect ratio	12.00
b	Wing span	1.5000 m
$\bar{c}$	Mean aerod. chord	0.1346 m
S	Wing area	0.1875 m²
q	Free stream dynamic pressure	
C_D	Drag/qS	
C_L	Lift/qS	
C_m	Pitching moment/qS$\bar{c}$	
C_ℓ	Rolling moment/qSb	
C_n	Yawing moment/qSb	
C_F	Net propeller thrust/qS	
	Wind referred axis system, moments referred to 25% MAC in fuselage center	
n	Propeller rotational speed rpm	
α	Angle of attack	
β	Angle of yaw	
δ_E	Elevator angle	
δ_F	Flap angle	
δ_A	Aileron angle	
δ_R	Rudder angle	